Characteristics of the East Asian Winter Climate Associated with the Westerly Jet Stream and ENSO

Song Yang, K.-M. Lau, and K.-M. Kim

NASA/Goddard Space Flight center

Laboratory for Atmospheres

Greenbelt, MD 20771, USA

August 2000

ABSTRACT

In this study, the influences of the East Asian jet stream (EAJS) and El Niño/Southern Oscillation (ENSO) on the interannual variability of the East Asian winter climate are examined with a focus on the relative climate impacts of the two phenomena. Although the variations of the East Asian winter monsoon and the temperature and precipitation of China, Japan, and Korea are emphasized, the associated changes in the broad–scale atmospheric circulation patterns over Asia and the Pacific and in the extratropical North Pacific sea surface temperature (SST) are also investigated.

It is demonstrated that there is no apparent relationship between ENSO and the interannual variability of EAJS core. The EAJS and ENSO are associated with distinctly different patterns of atmospheric circulation and SST in the Asian–Pacific regions. While ENSO causes major climate signals in the Tropics and over the North Pacific east of the dateline, the EAJS produces significant changes in the atmospheric circulation over East Asia and western Pacific. In particular, the EAJS explains larger variance of the interannual signals of the East Asian trough, the Asian continental high, the Aleutian low, and the East Asian winter monsoon. When the EAJS is strong, all these atmospheric systems intensify significantly.

The response of surface temperature and precipitation to EAJS variability and ENSO is more complex. In general, the East Asian winter climate is cold (warm) and dry (wet) when the EAJS is strong (weak) and it is warm during El Niño years. However, different climate signals are found during different La Niña years. In terms of linear correlation, both the temperature and precipitation of northern China, Korea, and central Japan are more significantly associated with the EAJS than with ENSO.

1. Introduction

It has been known that both the East Asian jet stream (EAJS) and El Niño/Southern Oscillation (ENSO) are important phenomena affecting the winter climate of East Asia and the western Pacific. During the past several decades, substantial efforts have been devoted to investigating the structure, maintenance, and variability of the EAJS as well as its impact on the weather and climate in many Asian countries and their adjacent regions (e.g., Bolin 1950; Hsieh 1951; Smagorinsky 1953; Mohri 1959; Yeh et al. 1959; Krishnamurti 1961; Reiter 1963; Zhu 1966; Palmén and Newton 1969; Zeng 1979; Huang and Gambo 1982; Wallace 1983; Gao and Tao 1991; Liang and Wang 1998). Previous studies have shown that the EAJS is associated closely with cyclogenesis, frontogenesis, blocking, and storm track activity on the synoptic time scale and with orographic features and land–sea thermal contrast on longer time scales. It has also been shown that the EAJS is linked to variations of the Hadley circulation (Palmén 1951; Bjerknes 1966; Hou 1998) and thus tropical convective activities (Chang and Lau 1980; Hoskins and Karoly 1981; Webster 1981; Chang and Lum 1985; Kang and Held 1986; Lau and Boyle 1987; Yang and Webster 1990; Dong et al. 1999).

Since the 1980s, ENSO's impact on the East Asian climate has been investigated extensively (e.g., Rasmusson and Carpenter 1983; Tao and Chen 1987; Huang and Wu 1989; Li 1990; Ding 1992; Webster and Yang 1992; Tomita and Yasunari 1996; Zhang et al. 1996; Kang 1997; Zhang et al. 1997; Cholaw and Ji 1999; Lau et al. 2000; Wang et al. 2000). Many studies have been conducted to understand the relationship between ENSO and the Asian monsoon and the role of ENSO in extreme weather and climate events such as serious floods/droughts and persistent cold/warm episodes.

Nevertheless, many questions about the relationship among ENSO, the EAJS, and the Asian–Pacific climate remain unanswered. Firstly, what is the relationship between ENSO and the EAJS? The EAJS covers a wide range of longitudes over Asia and the Pacific and only the

portion over the central–eastern Pacific shows a significant relationship with ENSO. Although the increase in strength of the central–eastern Pacific westerlies during El Niño years has been considered the intensification and eastward shift of the EAJS (e.g., Rasmusson and Wallace 1983), how the EAJS core varies with ENSO remains unclear. Secondly, what are the factors that affect the year–to–year changes of the EAJS especially the jet core? Since the EAJS is strongly affected by internal dynamics, it may not be an easy task to establish a strong link between the jet stream and surface forcings. However, if the EAJS exerts a strong impact on climate, it is important to reveal an only moderate relationship between the EAJS and slowly–varying surface forcings like sea surface temperature (SST). As discussed by previous studies (e.g., Lau and Nath 1990, 1996; Ting and Wang 1997; Robinson 2000), features of the connection between the atmospheric circulation and SST in the extratropics are far from being conclusive. Another important question that should be answered is about the relative influences of the EAJS and ENSO on the East Asian and Pacific climate. For any particular climate signal observed, how much of it is caused by the EAJS and how much is produced by ENSO? Although it is difficult to separate the influences by ENSO and the EAJS, the relative contributions of the two phenomena to a specific climate signal can be assess with certain confidence if an orthogonal relationship exists between the EAJS and ENSO.

In this study, we attempt to obtain useful information for answering the above questions. We will examine the interannual relationship between ENSO and the EAJS. We will explore how ENSO and the EAJS are connected to the atmospheric circulation patterns over the Asian–Pacific regions. Our focus will be placed on the changes of atmospheric circulation systems and Pacific SST associated with ENSO and the EAJS. We will also emphasize on the response of the East Asian winter monsoon and the temperature and precipitation of Asian countries to ENSO and the variability of the EAJS.

This paper is laid out as follows. In section 2, major features of the data sets used are

described. In section 3, we discuss the relationship between the EAJS and ENSO and compare the atmospheric teleconnection patterns and SST distributions that are associated with the two phenomena. The relative impacts of the EAJS and ENSO on the interannual variability of East Asian winter climate measured by temperature and precipitation fields are discussed in section 4. Finally, the study is summarized in section 5.

2. Data sets

The primary data used in this study are the winds and geopotential height from the reanalysis product of the US NOAA National Centers for Environmental Prediction (NCEP) and National Center for Atmospheric Research (NCAR). Other data sets include the NCEP Climate Prediction Center Merged Analysis of Precipitation (CMAP), NCEP reconstructed SST, and the surface air temperature (Ts) from the US NASA Goddard Institute for Space Studies (GISS). To depict detailed, regional climate features, we also analyze the station data precipitation and surface air temperature from China, Japan, and Korea (data obtained from ftp://ftp.ncdc.noaa.gov/pub/data/ghcn/v2; Peterson and Vose 1997). In addition, Southern Oscillation Index (SOI), the normalized difference in sea level pressure between Tahiti and Darwin, is applied in this study.

The horizontal resolutions of data are 2.5°x2.5° (latitude by longitude) for the NCEP/NCAR reanalyses (Kalnay et al. 1996) and CMAP precipitation (Xie and Arkin 1997), and 2°x2° for the GISS Ts (Hansen et al 1999) and NOAA SST (Smith et al. 1996). Because of the limitation in data availability, different periods of the data sets (1949–99 for NCEP/NCAR reanalyses, 1950–98 for GISS Ts, 1979–99 for CAMP precipitation, and 1950–99 for NCEP SST) are analyzed. The analyses of this work are all based on monthly values from which seasonal means are computed.

3. Broad-scale characteristics

It can be seen from Fig. 1a, which shows the 1949–99 December–February (DJF) climatology of U200, that the EAJS is one of the major atmospheric circulation systems over the Northern Hemisphere during winter. The EAJS is the strongest westerly jet stream with a maximum zonal wind speed greater than 70 ms^{-1} over the ocean immediately to the south of Japan (around 32.5°N, 140°E). In spite of its intensity, the center of EAJS does not vary substantially from year to year in both magnitude and location, due probably to the effect of the Tibetan Plateau (Ramage 1952). The standard deviation of the DJF EAJS maximum is 4 ms^{-1}, about one half of that of the westerlies over subtropical central North Pacific. Out of the total 50 DJFs from 1949 to 1999, the maximum of EAJS appears over 32.5°N,140°E 15 times. Latitudinally, it is located over 32.5°N 44 times and shifts southward to 30°N once and northward to 35°N five times. Longitudinally, the maximum of EAJS is usually located within 135–150°E, mostly appearing over 140°E or two grids (5 degrees) to the east or west of the longitude.

One of the important features of Fig. 1 is that the variations of the EAJS maximum are not strongly related to ENSO (Fig. 1b). Indeed, the simultaneous DJF correlation between SOI and the grid-point U200 is close to zero near the EAJS core. The largest westward shift (DJFs of 1950/51 and 1968/69) and eastward movement (DJFs of 1960/61 and 1986/87) of the EAJS occur irrelevantly to ENSO events. (While 1968/69 and 1986/87 are El Niño years, 1950/51 and 1960/61 are, respectively, La Niña and non-ENSO years.) In addition, neither of the two seasons during which the EAJS is the strongest (80 ms^{-1} in DJF of 1976/77 and 82 ms^{-1} in DJF of 1980/81) is an ENSO winter. On the other hand, besides the U200 over many tropical regions, the westerlies over the subtropical central-eastern Pacific are significantly correlated with ENSO. The strong relationship between these westerlies and ENSO often overshadows the relationship between ENSO and the East Asian-Pacific jet stream.

The weak relationship between ENSO and the EAJS core suggests that the two phenomena

may play different roles in modulating the climate of the East Asian and Pacific regions. It also demonstrates the need of measuring the variability of EAJS and assessing its climate impact appropriately. The small migration of the EAJS core facilitates the construction of an index that measures the jet stream. We define this index as the yearly DJF U200 averaged within 30–35°N and 125–165°E (see Fig. 1c), an area that covers the EAJS core of all winters. There is no apparent relationship between this index and SOI, which is also shown in Fig. 1c, with a near-zero correlation between the two time series.

Figure 1d shows the correlation between the EAJS index and grid-point U200. The dominant feature of the figure is that the variability of EAJS is associated with a northwest-southeast oriented teleconnection pattern over Asia and the western-central Pacific. This pattern is nearly identical to the correlation pattern in which the EAJS index is replaced by the one-point U200 time series of the climatological jet core location (32.5°N, 142.5°E). The pattern of Fig. 1d differs substantially from the ENSO-related teleconnection pattern shown in Fig. 1b. Except for the Asian-Australian monsoon regions, the ENSO-related features are mainly confined to the east of the dateline, oriented in a north-south direction over the central-eastern Pacific. At the locations where SOI-U200 correlations are strongest, the EAJS-U200 correlations are among the weakest, and vice versa. The differences between Figs. 1b and 1d imply that the EAJS and ENSO are associated with two different modes of the atmospheric circulation over the Asian-Pacific-American regions. These two models are confirmed by calculations of the empirical orthogonal function (EOF) of DJF U200 (figures not shown). While the features of the first EOF mode are similar to those shown in Fig. 1b, and second EOF mode captures features similar to those shown in Fig. 1d.

In brief, the interannual variability of the center of East Asian jet stream is not strongly correlated with ENSO. Instead, the EAJS and ENSO are associated with two distinctly different circulation patterns over Asia and the Pacific. We will reveal the detailed features of these two

teleconnection patterns shortly and discuss their association with regional climate in the next section.

Figure 2 shows the regression patterns of 500 mb geopotential height (H500) against, respectively, the EAJS and SOI. During winter, one of the major circulation systems at 500–mb level is the East Asian trough, which is anchored along the east coast of East Asia and extends from the Sea of Okhotsk through Japan to the East China Sea. It can be seen from Fig. 2a that the trough deepens when the EAJS strengthens. Associated with the intensified EAJS and trough is an adjustment of the large–scale circulation system over Asia and the Pacific. H500 decreases significantly to the east and increases to the northwest of the trough. Such an adjustment is associated with a wave–train pattern that spans the entire extratropical Northern Hemisphere. Thus, the variation of EAJS is linked to a teleconnection pattern that also affects the climate outside the Asian–Pacific regions.

The variations of H500 that are associated with ENSO (Fig. 2b) differ clearly from those shown in Fig. 2a. Although ENSO produces very significant signals over the Tropics, it causes much smaller changes over extratropical Asia. In addition, the locations of ENSO–related centers of the H500 variance over the central Pacific and North America are further eastward, compared with those associated with the EAJS.

Figure 3a shows the pattern of regression of 850–mb wind vectors against the EAJS index and that of the correlation (shadings) between the EAJS and grid–point SST. Associated with a strong EAJS is a broad–scale cyclonic pattern over the North Pacific, with strong changes over the Aleutian Islands and the Gulf of Alaska. An intensifying EAJS also gives rise to a stronger Asian continent high and thus stronger winter monsoon in East Asia (see more detailed discussions in the next section). In addition, significant EAJS–related signals can also be seen over North America and the Atlantic. These changes in the atmospheric circulation link to anomalies in the fields of precipitation and temperatures, which will be shown in the next section.

Figure 3a also indicates that associated with a strong EAJS are negative SST anomalies in the subtropical North Pacific including the East China Sea, the Yellow Sea, and the Sea of Japan. Over the extratropical oceans, the wintertime atmospheric signals are characterized by barotropic nature. When the EAJS intensifies, the underneath near surface winds over 25–42°N become stronger (figures not shown). The intensifying surface wind causes strong mixing, evaporation, and probably upwelling in some coastal regions, and decreases the SST. A strong EAJS is linked to positive SST anomalies in the area from the tropical western Pacific to subtropical eastern Pacific. These anomalies are associated with the weakening of the northeasterly trade winds over the ocean domains.

ENSO is connected to lower tropospheric wind and SST patterns that are very different from those shown in Fig. 3a. It can be seen from Fig. 3b that ENSO links dominant signals in the Tropics, where only moderate features are accounted for by the EAJS. Over the North Pacific, a cyclonic pattern appears during El Niño years but its center shifts eastward compared with that shown in Fig. 3a. Significant difference exists over the Asian continent and extratropical western Pacific where the EAJS seems to exert a larger climate impact than ENSO does (also see discussion in the next section). The East Asian winter monsoon is weaker during El Niño years, mainly over the South China Sea, the East China Sea, and southern China. The weaker monsoon circulation is consistent with the smaller surface temperature gradients between the Asian continent and surrounding oceans.

4. Regional features

In this section, we will depict the relative influences of the EAJS and ENSO on the regional climate of East Asia and western Pacific that is measured by two basic fields: temperature and precipitation. Figure 4 shows the composite pattern of difference in DJF surface air temperature between strong and weak EAJS years (Fig. 4a) and that between El Niño and La Niña years (Fig.

4b). The dominant feature of Fig. 4a is the cooling over the mid–latitude East Asia and western Pacific and the warming in the high latitudes associated with a strong EAJS. When the jet stream is strong, apparent cooling occurs in China, Korea, Japan, and many Southeast Asian countries. As expected, ENSO causes much stronger signals over the tropical Pacific (Fig. 4b). Over Asia, warm conditions prevail during El Niño years (or cold conditions during La Niña years). A careful examination of the figure indicates that the change in Ts is more apparent in Fig. 4a than in Fig. 4b for East China, Korea, Japan, and their adjacent areas.

Shown in Fig. 5 are the composite patterns of precipitation variations associated with the EAJS and ENSO. A strong EAJS causes less precipitation in the middle latitudes and more precipitation in the lower latitudes over Asia and the western Pacific and produces opposite signals over the central Pacific. When the EAJS is strong, precipitation reduces clearly in eastern China, Korea, and central–southern Japan. The EAJS–related change in East and Southeast Asia shown in Fig. 5a is consistent with the intensification of the Hadley overturning (see Fig. 3a) that depresses (enhances) atmospheric convection in the extratropics (Tropics). This result is in agreement with that of Chang and Lau (1980) and Lau and Boyle (1987) who showed that a strong jet stream is associated with enhanced convective activities over the tropical western Pacific and maritime continent.

Although El Niño produces more precipitation over Northeast China, Korea, and the Asian land areas around 20°N, it mainly causes strong signals in the Tropics, e.g., enhanced precipitation over the equatorial central–eastern Pacific and reduced precipitation over South and Southeast Asia (Fig. 5b). Indeed, only relatively weaker, mixed ENSO–related signals appear over the subtropical–extratropical Asian continent.

We now examine the more regional features of the response of East Asian climate to ENSO and the variability of EAJS. Figure 6 displays an index that measures the interannual variability of the East Asian winter monsoon. The index is defined as the normalized values of the DJF 850–

mb meridional wind that is averaged over the domain of 20°–40°N, 100°–140°E. In the figure, the values associated with strong EAJS (solid bars), weak EAJS (open bars), El Niño (E), and La Niña (L) years are indicated. It can be seen that the monsoon is usually strong when the EAJS is strong, and vice versa. For example, among the 23 years of strong monsoon (negative values), the EAJS is stronger than normal in 16 years and weaker than normal in seven years. Among the 22 years of weak monsoon, the EAJS is weak in 16 years and strong in six years. For the period 1949–99, the correlation between the EAJS and the monsoon is significant with a coefficient of −0.51. Figure 6 also indicates that the variability of the monsoon is also linked to ENSO. During the eight El Niño years, the monsoon is weaker than normal in six years and stronger than normal in two years. However, during the 11 La Niña years, the monsoon is strong in six years and waek in five years. For the entire period examined, the correlation between the monsoon and SOI is weaker (R = −0.37) than the monsoon–EAJS correlation.

Figure 7 shows the year–to–year variations of the normalized surface temperature from stations of northern China, Korea, and central Japan (see figure captions for the list of the stations). As in Fig. 6, the values associated with strong EAJS, weak EAJS, El Niño, and La Niña years are indicated, respectively, by solid bars, open bars, E, and L. For the entire 50 years from 1950 to 1999, the coefficient of correlation between the EAJS with the temperature of China, Korea, and Japan is respectively −0.24, −0.55, and −0.60. In spite of the relatively weak correlation for China, these numbers are larger than the coefficients of correlation between SOI and the temperature, which are consecutively −0.17, −0.25, and −0.35. For all three regions, above–normal Ts occurs mostly during weak EAJS years. In addition, most of the below–normal Ts in both Korea and Japan appears when the EAJS is strong.

According to Fig. 7, the East Asian temperature has a stronger linear relationship with the EAJS than with ENSO. However, the figure also indicates that above–normal Ts appears during most of the major El Niño events (for Korea, similar to the result of Kang 1997) and that there is

no apparent relationship between Ts and La Niña events.

Similar to Fig. 7, Fig. 8 shows the variability of the normalized precipitation of northern China, Korea, and central Japan. Unlike Fig. 5 where the CMAP precipitation since 1979 is analyzed, Fig. 8 depicts precipitation variability since 1949. The most prominent feature of the figure is that the precipitation of these regions is strongly correlated with the EAJS but not with ENSO. The coefficients of correlation between the EAJS and precipitation are −0.51 for China, −0.70 for Korea, and −0.57 for Japan. The association between strong EAJS and weak precipitation (or between weak EAJS and strong precipitation) occurs more frequently than the opposite EAJS–precipitation relationship. On the contary, the SOI–precipitation correlation coefficients are only −0.05 for China, −0.21 for Korea, and −0.17 for Japan. The figure indicates that major ENSO events do not cause consistent precipitation anomalies in East Asian regions, except that six out of the eight Niño events are accompanied by above–normal precipitation in Korea.

5. Summary

In this study, the influences of the East Asian jet stream (EAJS) and ENSO on the interannual variability of the East Asian winter climate have been examined with a focus on the relative climate impacts of the two phenomena. Although the variations of the East Asian winter monsoon and the temperature and precipitation of China, Japan, and Korea have been emphasized, the associated changes in the broad–scale atmospheric circulation patterns over Asia and the Pacific and in the extratropical North Pacific SST have been investigated as well.

It has been demonstrated that there is no apparent relationship between ENSO and the interannual variability of EAJS core. The two phenomena, whose variations are similar to the two gravest modes of the EOF of the 200–mb zonal wind over Asia and the Pacific, are connected to distinctly different patterns of atmospheric circulation and SST distributions. ENSO causes major

climate signals in the Tropics and over the North Pacific east of the dateline. During El Niño years, the East Asia winter monsoon is usually weak, leading to a warm regional climate. However, there is no clear relationship between La Niña and the East Asian winter climate including the monsoon and temperature and precipitation fields. As a results, the linear correlation between ENSO and the East Asian climate is very weak, at least for the period 1949–99.

Compared to ENSO, the EAJS produces larger changes in the atmospheric circulation over East Asia and the western Pacific. In particular, the EAJS explains larger variance of the interannual signals of the East Asian trough, the Asian continental high, the Aleutian low, and the East Asian winter monsoon. When the EAJS is strong, all these atmospheric systems intensify significantly, and East Asia is characterized by a cold and dry winter climate. Opposite climate signals appear when the EAJS is weak. In terms of linear correlation, both the temperature and precipitation of East Asia regions such as northern China, Korea, and central Japan are more significantly associated with the EAJS than with ENSO.

It has been understood that ENSO accounts for only part of the anomalies of the Earth's climate. In East Asia, the impact of ENSO on the regional climate is only moderate even relatively weak. Therefore, limitation exists in the skills of predicting the climate based solely on ENSO. This study has demonstrated the importance of the EAJS for understanding the variability of the East Asian climate. It has also suggested that to improve the prediction of Asian climate, the EAJS should be considered as an important factor. This is particular so given that the variability of the EAJS is connected to the SST in extratropical western Pacific. Furthermore, the EAJS also causes variability in the climate of the eastern Pacific and North America (Yang et al. 2000). The jet stream acts like a atmospheric bridge in connecting the climate signals in Asia and America. New evidence of such a cross–Pacific teleconnection, linked to the Asian monsoon, has recently provided by Lau and Weng (2000). To gain a better understanding of the variations of

climate in the Asia–Pacific–America regions, it is necessary to conduct more investigations into the association between the EAJS and the North Pacific SST and into the impact of EAJS on the climate outside the Asian and western Pacific regions.

References

Bjerknes, J. 1966, A possible response of the atmospheric Hadley circulation to equatorial anomalies of ocean temperature. *Tellus,* **18,** 820–829.

Bolin, B., 1950: On the influence of the earth's orography on the general character of the westerlies. *Tellus,* **2,** 184–196.

Chang, C.–P., and K. G. Lum, 1985: Tropical–midlatitude interactions over Asia and the western Pacific Ocean during the 1983–84 northern winter. *Mon. Wea. Rev.,* **113,** 1345–1358.

Cholaw B, and L. Ji, 1999: The ocean–atmosphere coupled regimes and East Asian winter monsoon (EAWM) activity. *Adv. Atmos. Sci.,* **16,** 91–106.

Ding, Y.–H., 1992: Summer monsoon rainfalls in China. *J. Meteor. Soc. Japan,* **70,** 373–396.

Dong, M., J. Yu, and S. Gao, 1999: A study on the variations of the westerly jet over East Asia and its relation with the tropical convective heating. *Chinese J. Atmos. Sci.,* **23(1),** 62–70.

Gao, S., and S. Tao, 1991: Acceleration of upper–tropospheric jet stream and lower–tropospheric frontogenesis. *Chinese J. Atmos. Soc.,* **15(2),** 11–21.

Hansen, J., R. Ruedy, J. Glascoe, and M. Sato, 1999: GISS analysis of surface temperature change. *J. Geophys. Res.,* **104,** 30997–31022.

Hoskins, B. J., and D. J. Karoly, 1981: The steady linear response of a spherical atmosphere to thermal and orographic forcing. *J. Atmos. Sci.,* **38,** 1179–1196.

Hou, A. Y., 1998: Hadley circulation as a modulator of the extratropical climate. *J. Atmos. Sci.,* **55,** 2437–2457.

Hsieh, Y. P., 1951: On the wind and temperature fields over western Pacific and estern Asia in winter. *J. Chinese Geophys. Soc.,* **2(3),** 279–297.

Huang, R., and K. Gambo, 1982: The response of a hemispheric multilevel model atmosphere to forcing by topography and stationary heat sources. *J. Meteor. Soc. Japan,* **60,** 78–108.

Huang, R., and Y. Wu, 1989: The influence of ENSO on the summer climate change in China

and its mechanism. *Adv. Atmos. Sci.*, **6**, 21–32.

Kalnay, E., M. Kanamitsu, R. Kistler, W. Collins, D. Deaven, L. Gandin, M. Iredell, S. Saha, G. White, J. Woollen, Y. Zhu, M. Chelliah, W. Ebisuzaki, W. Higgins, J. Janowiak, K. C. Mo, C. Ropelewski, J. Wang, A. Leetmaa, R. Reynolds, R. Jenne, and D. Joseph, 1996: The NCEP/NCAY 40–Year Reanalysis Project. *Bull. Amer. Meteor. Soc.*, **77**, 437–471.

Kang, I.–S., 1997: Effects of El Niño on Korean peninsula. Proceedings of El Niño Workshop. Korean Meteorological Administration, pp 27–40 (in Korean).

Kang, I.–S., and I.–M. Held, 1986: Linear and nonlinear diagnostic models of stationary eddies in the upper troposphere during northern summer. *J. Atmos. Sci.*, **43**, 3045–3057.

Krishnamurti, T. N., 1961: The subtropical jet stream of winter. *J. Meteor.*, **18**, 172–191.

Lau, K.–M., and J. S. Boyle, 1987: Tropical and extratropical forcing of the large–scale circulation: A diagnostic study. *Mon. Wea. Rev.*, **115**, 400–428.

Lau, K.–M., K.–M. Kim, and S. Yang, 2000: Dynamical and boundary forcing characteristics of regional components of the Asian summer monsoon. *J. Climate,* in press.

Lau, K.–M., and H. Weng, 2000: Teleconnection linking summertime droughts and floods over North America to the Asian/Pacific monsoon. *Nature,* submitted.

Lau, N.–C., and M. J. Nath, 1990: A general circulation model study of the atmospheric response to extratropical SST anomalies observed in 1950–79. *J. Climate,* **3**, 965–989.

Lau, N.–C., and M. J. Nath, 1996: The role of the "atmospheric bridge" in linking tropical Pacific ENSO events to extratropical SST anomalies. *J. Climate,* **9**, 2036–2057.

Li, C., 1990: Interaction between anomalous winter monsoon in East Asia and El Niño events. *Adv. Atmos. Sci.*, **7**, 36–46.

Liang, X.–Z., and W.–C. Wang, 1998: Associations between China monsoon rainfall and tropospheric jets. Quart. J. Roy. Meteor. Soc., 124, 2597–2623.

Mohri, K., 1959: Jet streams and upper fronts in the general circulation and their characteristics over the Far East (Part II). *Geophys. Mag.*, **29,** 333–412.

Palmén, E., 1951: The role of atmospheric disturbances in the general circulation. *Quart. J. Roy. Meteor. Soc.*, **77,** 337–354.

Palmén, E., and C. W. Newton, 1969: Atmospheric Circulation Systems: Their Structure and Physical Interpretation. Academic Press, Inc., San Diego, California, pp. 603.

Peterson, T. C., and R. S. Vose, 1997: An overview of the Global Historical Climatology Network temperature database. *Bull. Amer. Meteor. Soc.*, **78,** 2837–2849.

Ramage, C. S., 1952: Relationship of general circulation to normal weather over southern Asia and the western Pacific during the cool season. *J. Meteor.*, **9,** 403–408.

Rasmusson, E. M., and T. H. Carpenter, 1983: The relationship between the eastern Pacific sea surface temperature and rainfall over India and Sri Lanka. *Mon. Wea. Rev.*, **111,** 517–528.

Rasmusson, E. M., and J. M. Wallace, 1983: Meteorological aspects of the El Niño–Southern Oscillation. *Science,* **222,** 1195–1202.

Reiter, E. R., 1963: Jet–Stream Meteorology. Univ. of Chicago Press, Chicago, Illinois, pp. 515.

Robinson, W. A., 2000: Review of WETS–The workshop on extra–tropical SST anomalies. *Bull. Amer. Meteor. Soc.*, **81,** 567–577.

Smagorinsky, J., The dynamical influence of large–scale heat sources and sinks in the quasi–stationary mean motions of the Atmosphere. *Quart. J. Roy. Meteor. Soc.*, **79,** 342–366.

Smith, T. M., R. W. Reynolds, R. E. Livezey, and D. C. Stokes, 1996: Reconstruction of historical sea surface temperatures using empirical orthogonal functions. *J. Climate,* **9,** 1403–1420.

Tao, S.–Y., and L.–X. Chen, 1987: A review of recent research of the east Asian summer monsoon in China. In *Monsoon Meteorology,* Ed. By C.–P. Chang and T. N. Krishnamurti, Oxford Univ. Press, pp. 60–92.

Ting, M., and H. Wang, 1997: Summertime US precipitation variability and its relation to Pacific sea surface temperature. *J. Climate,* **10,** 1853–1873.

Tomita, T., and T. Yasunari, 1996: Role of the northeast winter monsoon on the biennial oscillation of the ENSO/monsoon system. *J. Meteor. Soc. Japan,* **74,** 399–413.

Wallace, J. M., 1983: The climatological mean stationary waves: Observational evidence. In *Large–Scale Processes in the Atmosphere*, Ed. By B. J. Hoskins and P. R. Pearce, pp. 27–52.

Wang, B., R. Wu, and X. Fu, 2000: Pacific–East Asian teleconnection: How does ENSO affect East Asian climate? *J. Climate,* **13,** 1517–1536.

Webster, P. J., 1981: Mechanisms determining the atmospheric response to sea surface temperature anomalies. *J. Atmos. Sci.,* **38,** 554–571.

Webster, P. J., and S. Yang, 1992: Monsoon and ENSO: Selectively interactive systems. *Quart. J. Roy. Meteor. Soc.,* **118,** 877–926.

Xie, P., and P. A. Arkin, 1997: Global precipitation: A 17–year monthly analysis based on gauge observations, satellite estimates and numerical model outputs. *Bull. Amer. Meteor. Soc.,* **78,** 2539–2558.

Yang, S., K.–M. Lau, and K.–M. Kim, 2000: Wintertime East Asian jet stream and its association with the Asian–Pacific climate. *J. Climate,* submitted.

Yang, S., and P. J. Webster, 1990: The effect of summer tropical heating on the location and intensity of the extratropical westerly jet streams. *J. Geophys. Res.,* **95,** 18705–18721.

Yeh, T.–C., S.–Y. Dao, and M.–T. Li, 1959: The abrupt change of circulation over the Northern Hemisphere during June and October. In *The Atmosphere and the Sea in Motion,* Ed. By B. Bolin, Rockefeller Inst. Press, New York, pp. 249–267.

Zeng, Q. C., 1979: Mathematical and Physical Basis for Numerical Weather Forecast. Science Press, Beijing, China, pp. 314.

Zhang, R., A. Sumi, and M. Kimoto, 1996: Impact of El Nio on the East Asian monsoon: A diagnostic study of the '86/87 and '91/92 events. *J. Meteor. Soc. Japan,* **74,** 49–62.

Zhang, Yi, K. R. Sperber, and J. S. Boyle, 1997: Climatology and interannual variation of the East Asian winter monsoon: Results from the 1979–95 NCEP/NCAR reanalysis. *Mon. Wea. Rev.,* **125,** 2605–2619.

Zhu, B., 1966: Atmospheric circulation and weather in Southeast and South Asia. Beijing Scientific Press, pp.

Figure captions

Fig. 1. (a) 1949–1999 climatology of DJF U200 (ms^{-1}) from NCEP/NCAR reanalysis product. Values ≥ 40 ms^{-1} are shaded. (b) DJF correlation between SOI and the U200 at each grid for the period from 1949 to 1999. (c) Normalized time series of the EAJS (DJF U200 averaged over 30–35°N, 125–165°E) and SOI. The correlation between the two time series has a coefficient of 0.05. (d) DJF correlation between the EAJS and the U200 at each grid for the period from 1949 to 1999. Values ≥ 99% confidence level are shaded in (b) and (d).

Fig. 2. Regressions (in m) of the DJF 500–mb geopotential height (H500) against the EAJS (a) and against negative SOI (b). Shadings indicate the areas where the correlation of H500 with EAJS (or with SOI) is significant at the 99% confidence level.

Fig. 3. Vectors represent regressions (in ms^{-1}) of the DJF 850–mb winds against the EAJS (a) and negative SOI (b). The shadings indicate the correlation between the EAJS and SST (a), and between negative SOI and SST. Only the information that is statistically significant at 99% confidence level is shown in the figure.

Fig. 4. (a) Composite pattern of the difference in Ts (in °C) between strong and weak EAJS years. The strong EAJS category includes the DJFs of 1952/53, 61/62, 67/68, 69/70, 76/77, 80/81, 83/84, 94/95, and 95/96. The weak EAJ category includes the DJFs of 1953/54, 58/59, 68/69, 71/72, 72/73, 78/79, 89/90, 91/92, and 92/93. (b) Composite pattern of the difference in Ts between El Niño and La Niña years. The El Niño years include 1951/52, 57/58, 58/59, 72/73, 77/78, 82/83, 86/87, 91/92, and 97/98. The La Niña years include 1950/51, 55/56, 61/62, 66/67, 70/71, 73/74, 75/76, 88/89, and 96/97.

Fig. 5. (a) Composite pattern of the difference in precipitation percentage (divided by climatology) between strong and weak EAJS years. The strong EAJS category includes the DJFs of 1980/81, 83/84, 94/95, and 95/96. The weak EAJ category includes the DJFs of 1978/79, 89/90, 91/92, and 92/93. (b) Composite pattern of the difference in precipitation

percentage between El Niño and La Niña years. The El Niño years include 1982/83, 86/87, 91/92, and 97/98. The La Niña years include 1981/82, 88/89, 96/97, and 98/99.

Fig. 6. East Asian winter monsoon index defined as the normalized area–averaged values of the meridional component of DJF 850–mb winds (ms^{-1}) ove (20°–40°N, 100°–140°E). The values of strong and weak EAJS years are shown by solid and open bars, respectively. The letters E and L stand for El Niño and La Niña. The coefficients are −0.51 for the EAJS–monsoon correlation and −0.37 for the SOI–monsoon correlation. The label 1950 in x–coordinate represents the season from December 1949 to February 1950.

Fig. 7. Normalized DJF surface temperature for (a) Chinese stations (Beijing, Qingdao, Shenyang, Taiyuan, and Yinchuan), (b) Korean stations (Kangnung, Mokpo, Pusan, Seoul, and Taegu), and (c) Japanese stations (Kanazawa, Nagoya, Osaka, Shionomisaki, and Tokyo). The values of strong and weak EAJS years are shown by solid and open bars, respectively. The letters E and L stand for El Niño and La Niña. The EAJS–temperature (SOI–temperature) correlation coefficients are −0.24 (−0.17) for China, −0.55 (−0.25) for Korea, and −0.60 (−0.35) for Japan.

Fig. 8. Normalized DJF precipitation for (a) Chinese stations (Beijing, Qingdao, Shenyang, Taiyuan, and Yinchuan), (b) Korean stations (Kangnung, Mokpo, Pusan, Seoul, and Taegu), and (c) Japanese stations (Kanazawa, Nagoya, Osaka, Shionomisaki, and Tokyo). The values of strong and weak EAJS years are shown by solid and open bars, respectively. The letters E and L stand for El Niño and La Niña. The EAJS–precipitation (SOI–precipitation) correlation coefficients are −0.51 (−0.05) for China, −0.70 (−0.21) for Korea, and −0.57 (−0.17) for Japan.

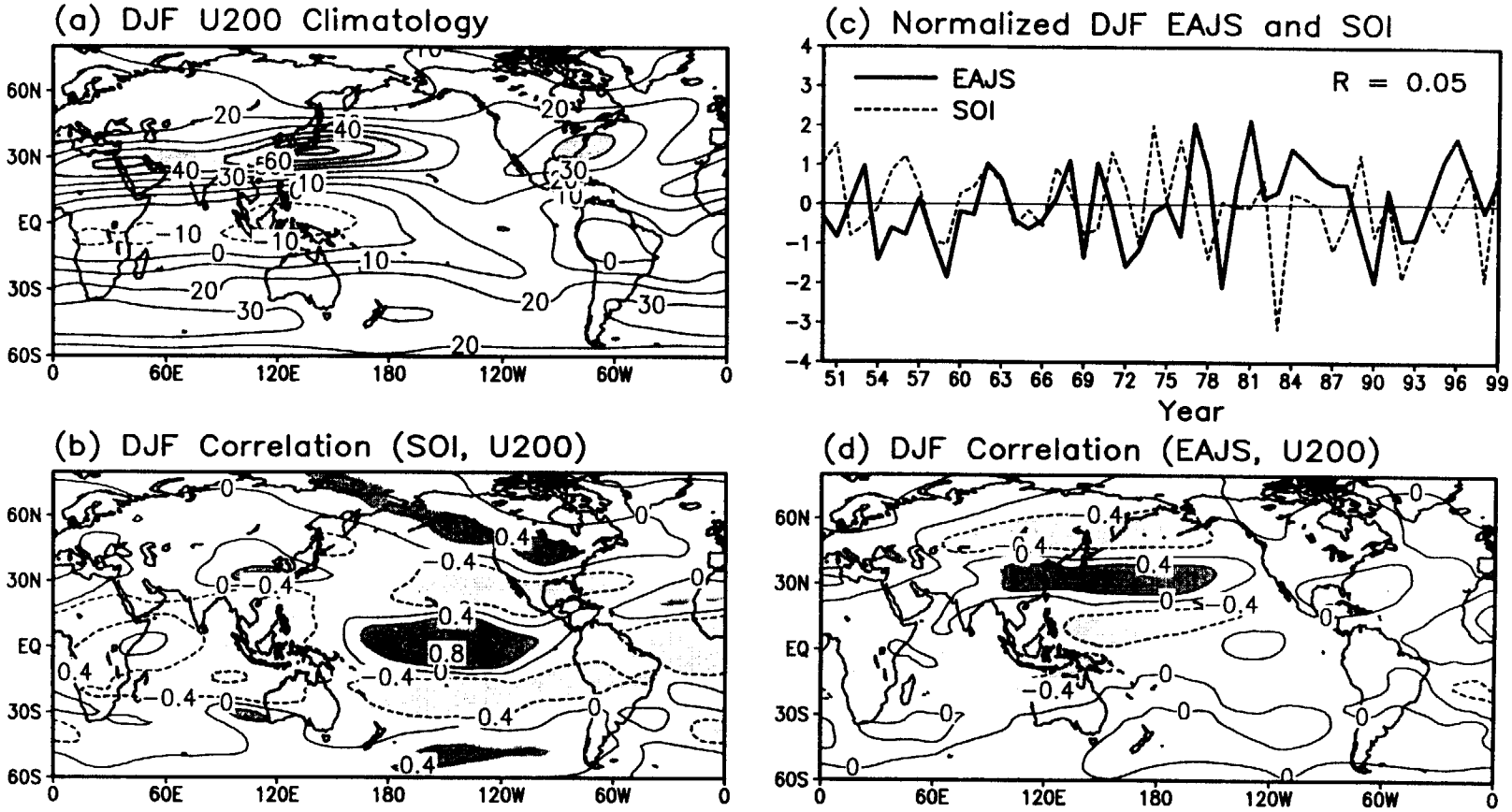
(a) DJF U200 Climatology
60N
30N
EQ
30S
60S
0
60E
120E
180
120W
60W
(c) Normalized DJF EAJS and SOI
EAJS
SOI
R = 0.05
Year
(b) DJF Correlation (SOI, U200)
(d) DJF Correlation (EAJS, U200)

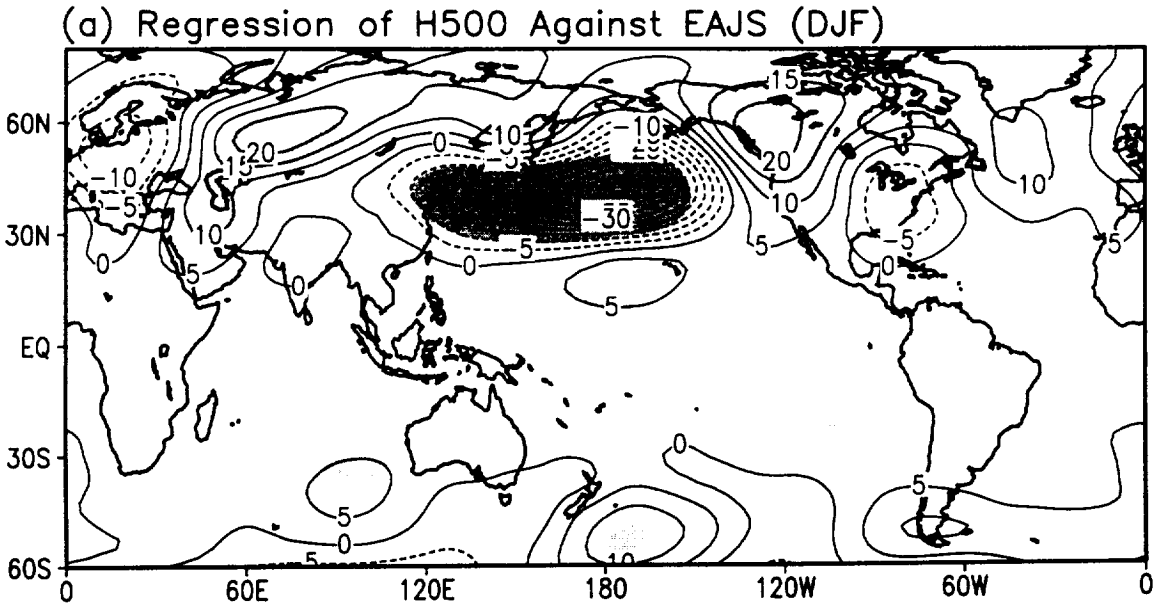
(a) Regression of H500 Against EAJS (DJF)
60N
30N
EQ
30S
60S
0
60E
120E
180
120W
60W
0

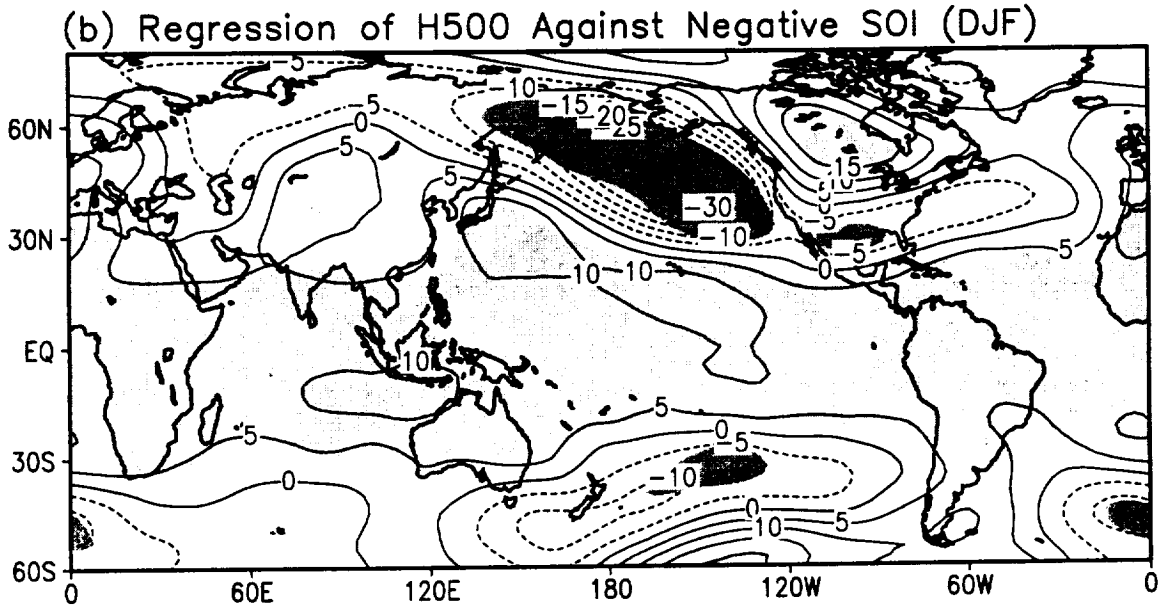
(b) Regression of H500 Against Negative SOI (DJF)
60N
30N
EQ
30S
60S
0
60E
120E
180
120W
60W
0

(a) EAJS Related SST and 850−mb Wind Patterns

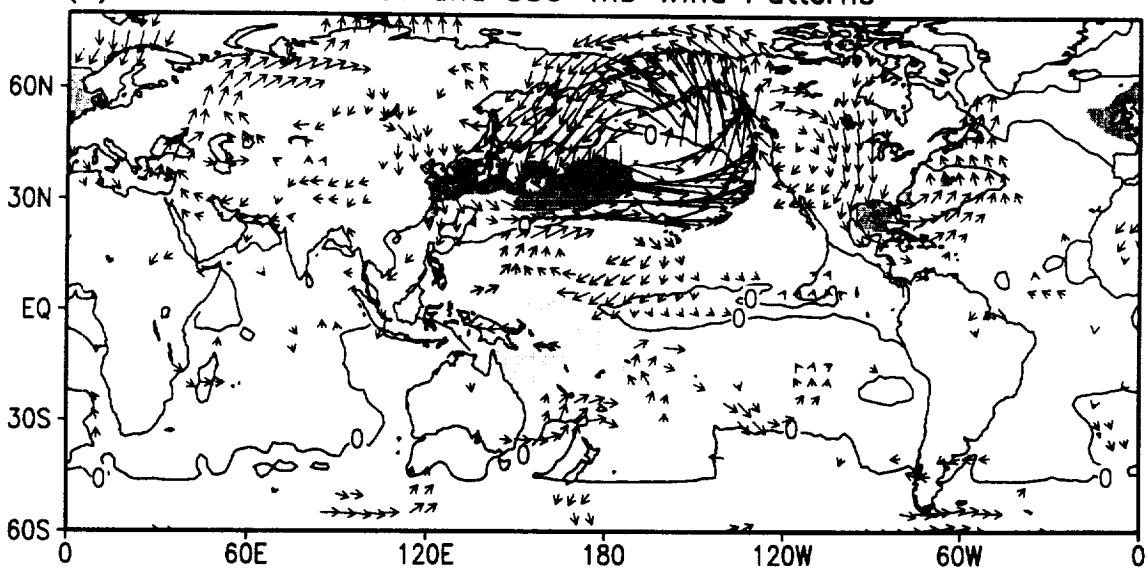

2

(b) Negative SOI Related SST and 850−mb Wind Patterns

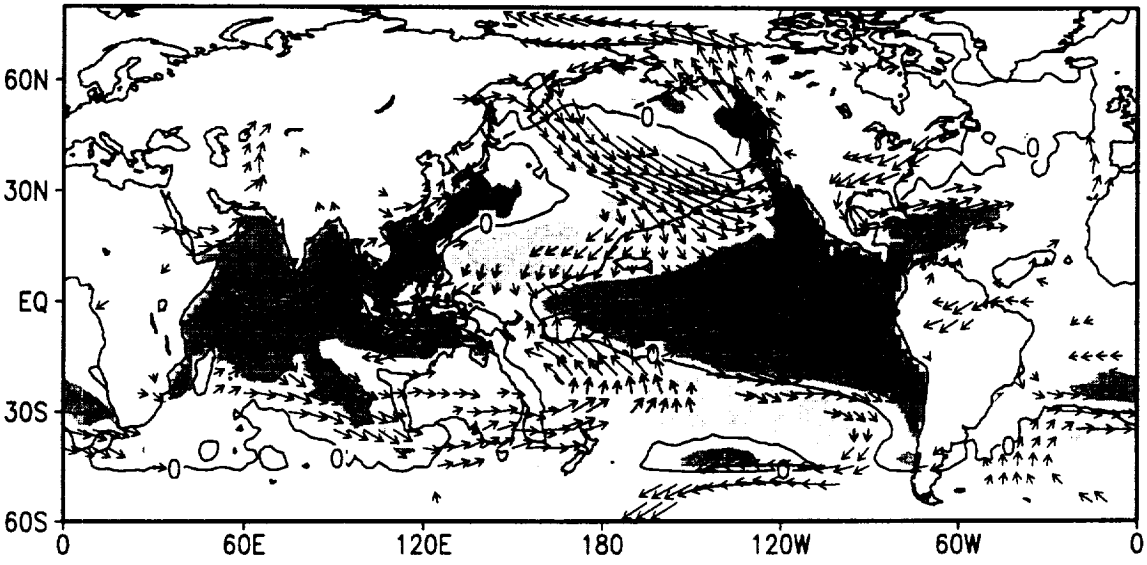

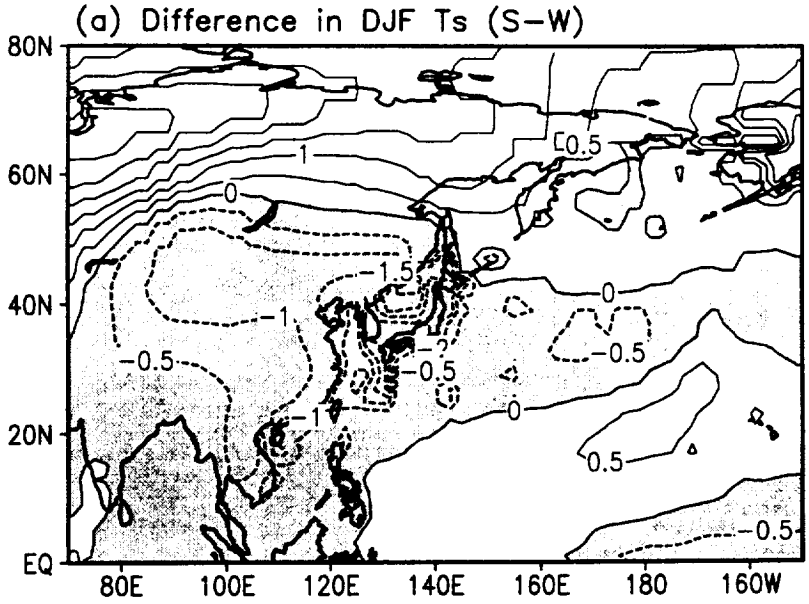
(a) Difference in DJF Ts (S−W)
80N
60N
40N
20N
EQ
80E
100E
120E
140E
160E
180
160W
1
0.5
0
1.5
-1
-0.5
-2
-0.5
0
-0.5
-1
0
0.5
-0.5

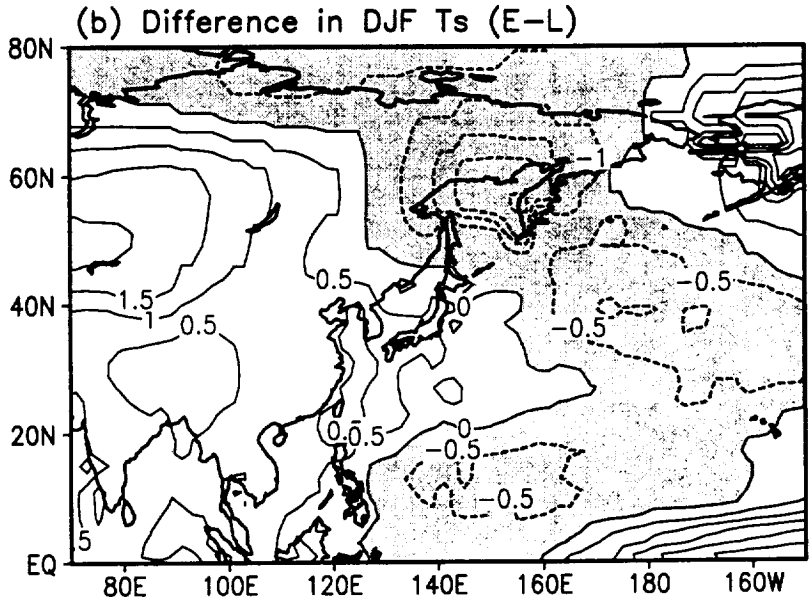
(b) Difference in DJF Ts (E−L)
80N
60N
40N
20N
EQ
80E
100E
120E
140E
160E
180
160W
-1
0.5
-0.5
1.5
1
0.5
0
-0.5
0.5
0
-0.5
-0.5
5

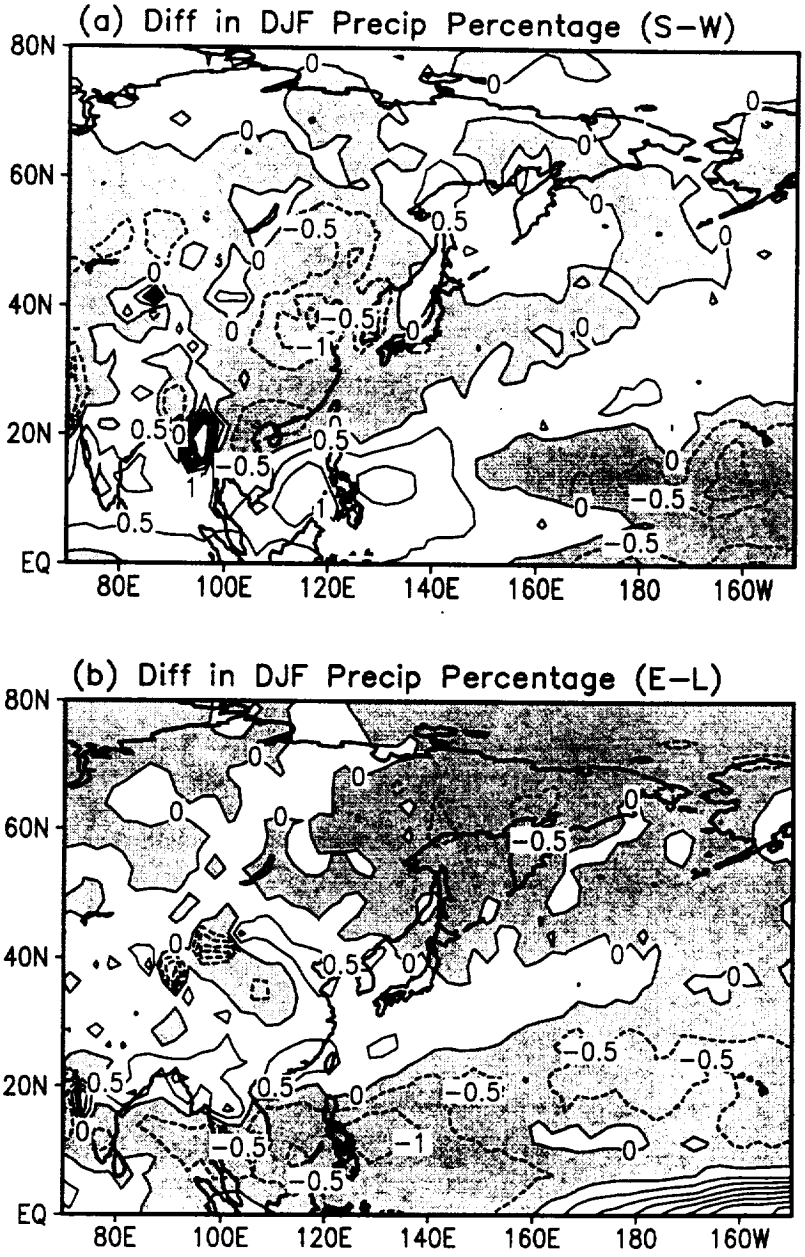
(a) Diff in DJF Precip Percentage (S−W)
80N
60N
40N
20N
EQ
80E
100E
120E
140E
160E
180
160W
(b) Diff in DJF Precip Percentage (E−L)
80N
60N
40N
20N
EQ
80E
100E
120E
140E
160E
180
160W

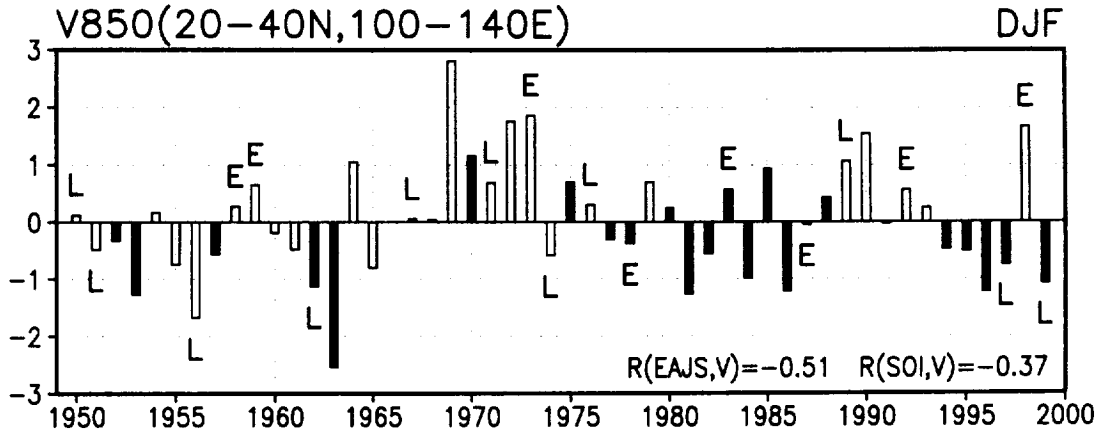
V850(20−40N,100−140E)
DJF
3
2
1
0
−1
−2
−3
1950
1955
1960
1965
1970
1975
1980
1985
1990
1995
2000
R(EAJS,V)=−0.51 R(SOI,V)=−0.37

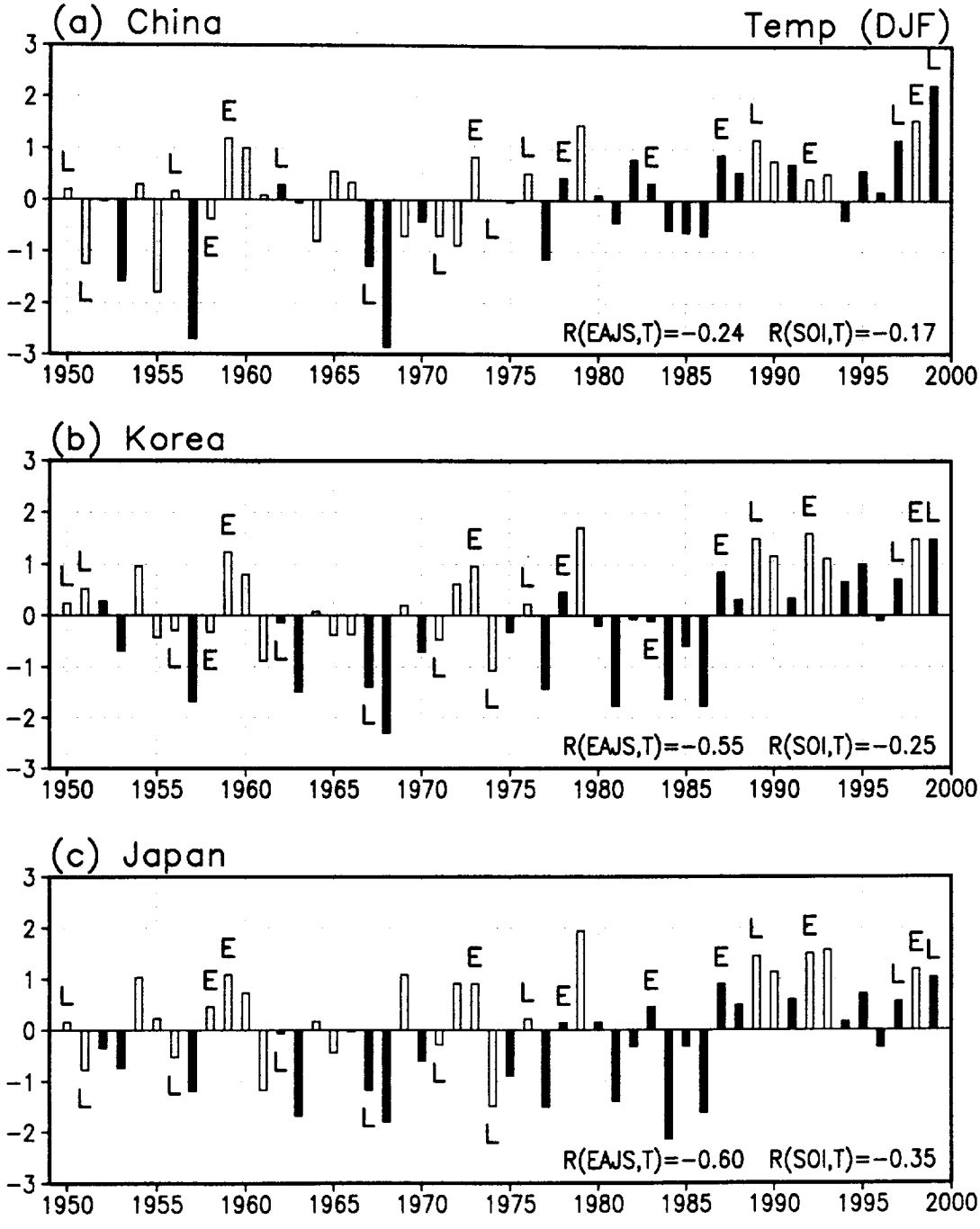
(a) China
Temp (DJF)
R(EAJS,T)=−0.24 R(SOI,T)=−0.17
(b) Korea
R(EAJS,T)=−0.55 R(SOI,T)=−0.25
(c) Japan
R(EAJS,T)=−0.60 R(SOI,T)=−0.35
3
2
1
0
−1
−2
−3
1950
1955
1960
1965
1970
1975
1980
1985
1990
1995
2000

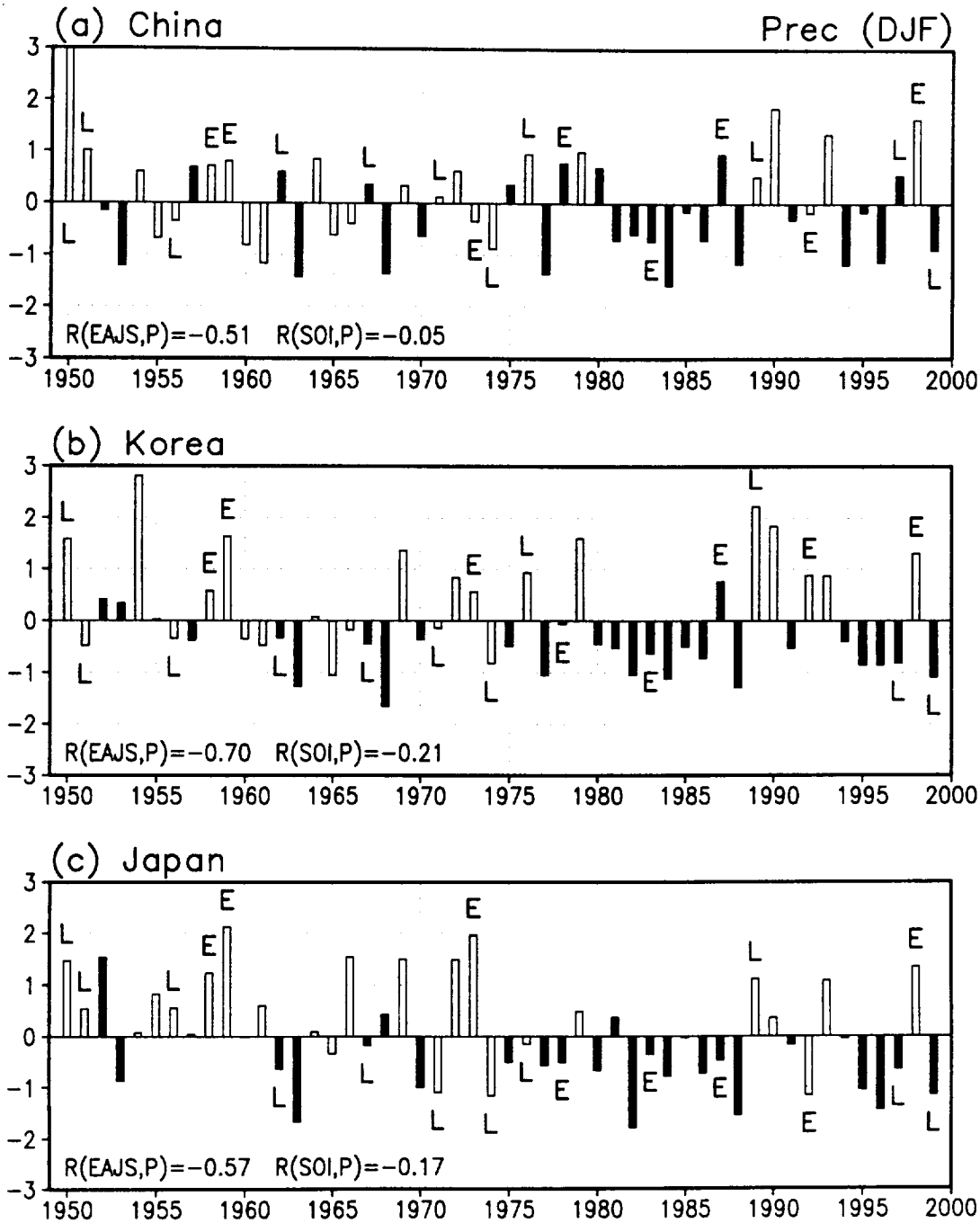
(a) China
Prec (DJF)
R(EAJS,P)=−0.51 R(SOI,P)=−0.05
(b) Korea
R(EAJS,P)=−0.70 R(SOI,P)=−0.21
(c) Japan
R(EAJS,P)=−0.57 R(SOI,P)=−0.17
3
2
1
0
−1
−2
−3
1950
1955
1960
1965
1970
1975
1980
1985
1990
1995
2000